Inorganic Chemistry

Article

pubs.acs.org/IC

Phase Evolution, Phase Transition, Raman Spectra, Infrared Spectra, and Microwave Dielectric Properties of Low Temperature Firing $(K_{0.5x}Bi_{1-0.5x})(Mo_xV_{1-x})O_4$ Ceramics with Scheelite Related Structure

Di Zhou,*[,†,‡] Li-Xia Pang,[§] Jing Guo,[†,‡] Hong Wang,[†,‡] Xi Yao,[†,‡] and Clive Randall[∥]

[†]Electronic Materials Research Laboratory, Key Laboratory of the Ministry of Education, Xi'an Jiaotong University, Xi'an 710049, Shaanxi, China

[‡]International Center for Dielectric Research, Xi'an Jiaotong University, Xi'an 710049. China

[§]Micro-optoelectronic Systems Laboratories, Xi'an Technological University, Xi'an 710032, Shaanxi, China

[∥]Center for Dielectric Studies, Materials Research Institute, Pennsylvania State University, University Park, Pennsylvania 16802, United States

ABSTRACT: In the present work, the $(K_{0.5x}Bi_{1-0.5x})(Mo_xV_{1-x})O_4$ ceramics ($0 \le x \le 1.00$) were prepared via the solid state reaction method and sintered at temperatures below 830 °C. At room temperature, the $BiVO_4$ scheelite monoclinic solid solution was formed in ceramic samples with $x < 0.10$. When x lies between 0.1−0.19, a $BiVO_4$ scheelite tetragonal phase was formed. The phase transition from scheelite monoclinic to scheelite tetragonal phase is a continuous, second order ferroelastic transition. High temperature X-ray diffraction results showed that this phase transition can also be induced at high temperatures about 62 °C for $x = 0.09$ sample, and has a monoclinic phase at room temperature. Two scheelite tetragonal phases, one being a $BiVO_4$ type and the other phase is a $(K,Bi)_{1/2}MoO_4$ type, coexist in the compositional range $0.19 < x < 0.82$. A pure $(K,Bi)_{1/2}MoO_4$ tetragonal type solid solution can be obtained in the range $0.82 \le x \le 0.85$. Between $0.88 \le x \le 1.0$, a $(K,Bi)_{1/2}MoO_4$ monoclinic solid solution region was observed. Excellent microwave dielectric performance with a relative dielectric permittivity around 78 and Qf value above 7800 GHz were achieved in ceramic samples near the ferroelastic phase boundary (at $x = 0.09$ and 0.10).

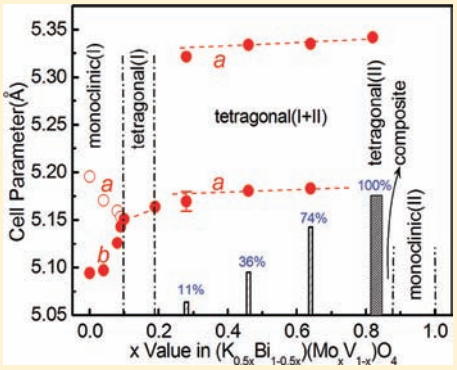

INTRODUCTION

With the development of wireless communication and microwave devices, microwave dielectric ceramics have been widely studied for more than forty years. Recently, the low temperature cofired ceramic (LTCC) technology has played an important role in the fabrication to meet the requirement of miniaturization and integration, such as in the modern iPhone. The LTCC requires the microwave dielectric ceramics to have a lower sintering temperature than the melting point of inner electrode materials, such as 961 °C for Ag and 1042 °C for Cu.[1,2]

Recently, $BiVO_4$ has attracted extensive interest for water decomposition and organics photocatalytic degradation.[3,4] Valant et al.[5] and Wee et al.[6] found that the $BiVO_4$ ceramic also possesses good microwave dielectric properties with a dielectric relative permittivity $\varepsilon_r \sim 68$, a quality factor Qf ~ 6500−8000 GHz, a temperature coefficient of resonant frequency TCF ~ −243 ~ −260 ppm/°C and a sintering temperature below 900 °C. Although the $BiVO_4$ was found to be thermochemically reactive with Ag,[5] in our previous study[7] it also was shown that there was limited interactions with Al and Cu electrode materials in $BiVO_4$-based scheelite solid solutions. The $(K_{0.5}Bi_{0.5})MoO_4$ ceramic was reported to show a distorted scheelite structure and a very low sintering temperature around 630 °C.[8,9] Hence, the introduction of $(K_{0.5}Bi_{0.5})MoO_4$ into $BiVO_4$ ($(K_{0.5}Bi_{0.5})^{2+}$ for A site and Mo^{6+} for B site) might lead to novel structures and dielectric properties. In the present work, the $(K_{0.5x}Bi_{1-0.5x})(Mo_xV_{1-x})O_4$ ceramics were prepared via the solid state reaction method. Then the phase evolution, phase transition, Raman spectra, and microwave dielectric properties of $(K_{0.5x}Bi_{1-0.5x})(Mo_xV_{1-x})O_4$ ceramics were studied and discussed.

EXPERIMENTAL SECTION

Proportionate amounts of reagent-grade starting materials of Bi_2O_3(>99%, Shu-Du Powders Co. Ltd., Chengdu, China), K_2CO_3(>99%, Sinopharm Chemical Reagent Co., Ltd., Shanghai, China), MoO_3(>99%, Fuchen Chemical Reagents, Tianjin,China) and V_2O_5 (>99%, Sinopharm Chemical Reagent Co., Ltd., Shanghai, China) were prepared according to the stoichiometric formulation $(K_{0.5x}Bi_{1-0.5x})(Mo_xV_{1-x})O_4$ compositions (x = 0, 0.04, 0.08, 0.09, 0.10, 0.19, 0.28, 0.46, 0.64, 0.82, 0.85, 0.86, 0.87, 0.88, 0.91, and 1.00, denoted as KBMVx). Powders were mixed and milled for 4 h using a planetary mill (Nanjing Machine Factory, Nanjing, China) by setting

Received: August 26, 2011
Published: November 21, 2011

 © 2011 American Chemical Society dx.doi.org/10.1021/ic201862e | *Inorg. Chem.* 2011, 50, 12733−12738

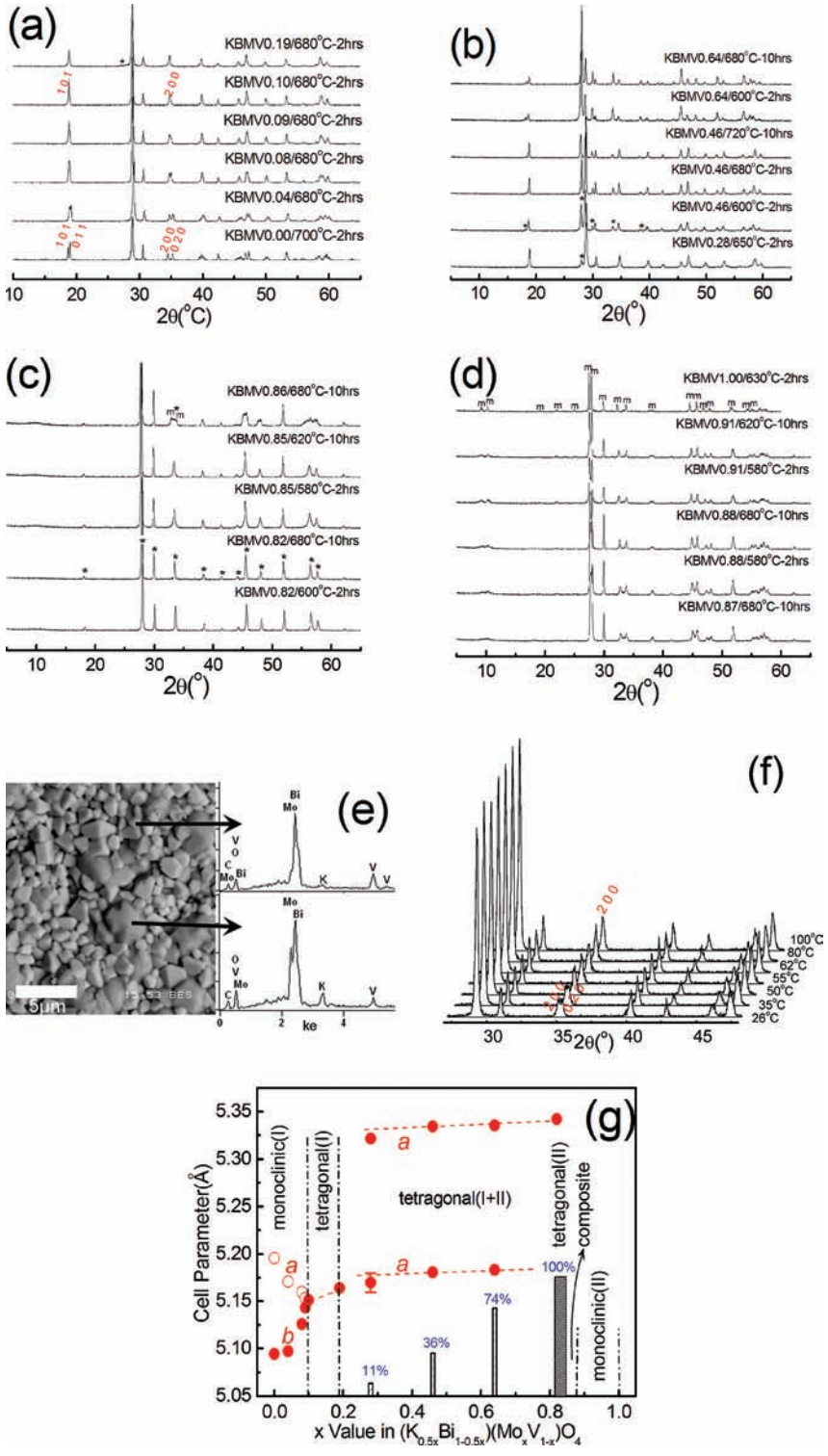

Figure 1. Room temperature XRD patterns of $(K_{0.5x}Bi_{1-0.5x})(Mo_xV_{1-x})O_4$ ceramics ($0 \leq x \leq 1.0$) sintered at different temperatures with different incubation time (a) (b) (c) (d), BEI and EDS analysis of KBMV0.46 (e), high temperature XRD patterns for $x = 0.09$ sample (f) (*, the secondary tetragonal phase, m-$(K,Bi)_{1/2}MoO_4$ type monoclinic phase) and cell parameters a and b of tetragonal phases as a function of x value ($x \leq 0.82$) (the bar charts represent the weight content of secondary tetragonal phase in KBMV0.28, KBMV0.46, KBMV0.64, and KBMV0.82 samples) (g).

the running speed at 150 rpm with the zirconia balls (2 mm in diameter) as milling media. The powder mixture was then dried and calcined at 580−680 °C for 4 hrs according to the composition. The calcined powders were ball milled again for 5 hrs with running speed at 200 rpm to obtain fine powders. Then powders were pressed into cylinders (12 mm in diameter and 5−6 mm in height) in a steel die with 5 wt. % PVA binder addition under a uniaxial pressure of 200 MPa. Samples were sintered in the temperature range from 600 to 800 °C for 2 hrs. Room temperature XRD was performed using a XRD with CuKa radiation (Rigaku D/MAX-2400 X-ray diffractometry, Tokyo, Japan). High temperature XRD was performed in the temperature range from room temperature to 110 °C using a XRD with CuKa radiation (XRD-7000, Shimadzu, Kyoto, Japan). Prior to examination sintered pellets were crushed in a mortar and pestle to

dx.doi.org/10.1021/ic201862e | Inorg. Chem. 2011, 50, 12733−12738

powder. Diffraction patterns were obtained between 15 and 65° (2θ) at a step size of 0.02°. To examine the grain morphology, as-fired surfaces were examined by scanning electron microscopy (SEM) (JSM-6460, JEOL, Tokyo, Japan). The Raman spectra at room temperature were obtained on polished pellets with a Raman spectrometer (inVia, Renishaw, England) excited with an Ar^+ laser (514.5 nm). The high temperature Raman spectra were measured using another Raman spectrometer (LabRAM HR800, HORIBA Jobin Yvon, France). The IR reflectivity spectra were measured using a Bruker IFS 66v FTIR spectrometer on Infrared beamline station (U4) at National Synchrotron Radiation Lab. (NSRL), China. Dielectric behaviors in the microwave frequency range were measured with the $TE_{01\delta}$ dielectric resonator method using a network analyzer (HP 8720 Network Analyzer, Hewlett-Packard) and a temperature chamber (Delta 9023, Delta Design, Poway, CA).

RESULTS AND DISCUSSIONS

The room temperature and high temperature XRD patterns of $(K_{0.5x}Bi_{1-0.5x})(Mo_xV_{1-x})O_4$ ceramics ($0 \leq x \leq 1.0$) sintered at different temperatures with different incubation times are shown in Figure 1 (a), (b), (c), and (d). In the range $0 \leq x < 0.19$, a gradually phase transition from the $BiVO_4$ monoclinic structure to scheelite tetragonal structure was observed, along with the characteristic splitting of (1 0 1) peak into (1 0 1) and (0 1 1) peaks, (2 0 0) peak splitting into (2 0 0) and (0 2 0) peaks etc., which is similar to the results in $(Li_{0.5x}Bi_{1-0.5x})(Mo_xV_{1-x})O_4$ system.[10,11] There exists a ferroelastic phase transition (reversible, second order) from a monoclinic (I2/a) to tetragonal ($I4_1/a$) phase in pure $BiVO_4$, as reported earlier by Bierlein et al., Sleight et al., and David et al.,[12−14] which can be induced by a high temperature about 255 °C or through an applied external pressure. To check the temperature sensitivity of the phase transition in the $(K_{0.5x}Bi_{1-0.5x})(Mo_xV_{1-x})O_4$ system, high temperature XRD was performed on the sample KBMV0.09, which shows a monoclinic structure at room temperature, and the results are shown in Figure 1 (f). The characteristic peak splitting was also observed in the high temperature XRD patterns of KBMV0.09 sample at around 62 °C, which indicates that the phase transition in $(K_{0.5x}Bi_{1-0.5x})(Mo_xV_{1-x})O_4$ ceramics has the same characteristic with pure $BiVO_4$ and confirms that that the ferroelastic-paraelastic phase transition temperature in the $(K_{0.5x}Bi_{1-0.5x})(Mo_xV_{1-x})O_4$ ceramics was shifted from 255 °C for pure $BiVO_4$ to 62 °C for samples with x =0.09.

From the XRD patterns of KBMV0.19 sample, a weak peak exists at about 2θ=28 °, which indicates the appearance of secondary phase. With the further increase of x value, it is clear that another set of peaks which also belong to a tetragonal structure becomes stronger and stronger, along with the weakening of the first set of tetragonal peaks. For KBMV0.46 sample sintered at 720 °C, which is near the melting point (partial melted at 720 °C), for 10 h, it is found that the two tetragonal phases coexisted and their ratio did not change comparing with the sample sintered at 600 °C for 2 h as shown in Figure 1(b), which means that the phase equilibrium can be easily achieved at a low temperature 600 °C for 2 h. It is assumed that x=0.19 and x=0.82 is the solid solubility limit for the first tetragonal phase and the secondary tetragonal phase, respectively. Hence, the KBMV0.46 sample was supposed to be composed of both KBMV0.19 and KBMV0.82 compositions (the atom weight is 316.4 and 291.2, respectively). Considering the conservation of elements as shown in the following equation:

$$\text{KBMV0.46} = y\text{KBMV0.19} + (1 - y)\text{KBMV0.82} \quad (1)$$

The mol ratio y is equal to $^4/_7$ = 0.57, which means that the mol percent of KBMV0.19 in the KBMV0.46 composite ceramic is about 57% and the weight percent is 59%. From the XRD patterns, the weight percent of KBMV0.19 in the composite is about 64%, which is similar to the calculated result from eq 1. Due to the similar compositions of KBMV0.19 and KBMV0.82, no color/contrast difference of grains can be observed from the BEI photo, but it is clear that there exist two kinds of grains in KBMV0.46 ceramic sample with different grain sizes as shown in Figure 1 (e). According to the EDS analysis, the larger grains (~5 μm) have much more Mo and K element contents than the smaller grains (~1 μm), which means the larger grains are associated to the secondary tetragonal phase KBMV0.82 and the smaller grains belong to the first tetragonal phase KBMV0.19. The content of the secondary tetragonal phase almost linearly increased as the x value increased in the region $0.28 \leq x \leq 0.82$ in composite samples as shown in the bar charts in Figure 1 (g).

Similar to the XRD results for KBMV0.46 sample, the two tetragonal phases were also observed in KBMV0.64 sample. When x reaches 0.82, only the secondary set of tetragonal phase peaks can be observed, which reveals that at this composition only one stable phase can be formed as shown in Figure 1 (c). The cell parameters of the first and secondary scheelite phases almost did not change with the composition in the range $0.28 \leq x \leq 0.82$ as seen from Figure 1 (g). However, the cell parameters for x = 0.28 composition deviated a little from the linear relation. This result can be attributed to the weak accuracy of the calculation of cell parameters caused by the small content of first scheelite phase and the uncertainty of solid solution limit.

It is seen that from the Figure 1 (c), the pure secondary scheelite phase can be kept stable even x value reached 0.85. In another word, the secondary scheelite phase solid solution was obtained in the range $0.82 \leq x \leq 0.85$. When x was bigger than 0.85 (for x = 0.86 and 0.87), a $(K_{0.5}Bi_{0.5})MoO_4$ type monoclinic phase appeared. For KBMV0.88, KBMV0.91, and KBMV1.00 (pure $(K_{0.5}Bi_{0.5})MoO_4$) samples, the scheelite phase was not formed here as shown in Figure 1 (d) and this result is similar to Klevtsov's report.[8] The real $(KBi)_{1/2}MoO_4$ ceramic crystallizes with a monoclinic space group $P2_1/c = C_{2h}^5$ with 12 molecules per unit-cell and is isostructural with α-$KSm(MoO_4)_2$.[15−17] Considering the Klevtsov and Vinokurov's high temperature XRD analysis,[18] the low temperature monoclinic phase of $(KBi)_{1/2}MoO_4$ continuously transitions to the high temperature tetragonal scheelite structure over a broad temperature range and is completed at 660 °C, which also has an order−disorder transiformation of K^+ and Bi^{3+} cations in the crystal structure. The pure tetragonal scheelite $(K,Bi)_{1/2}MoO_4$, which can be obtained by quenching samples from temperature 680−710 °C (melting point), and a transformation to the monoclinic irreversibly at a temperature 380 °C can be observed.[18] Different to the KBMV0.88, KBMV0.91, and KBMV1.00 samples, which both crystallized in the monoclinic structure, the pure secondary tetragonal phase was formed in the range $0.82 \leq x \leq 0.85$ and maintained its stability into the temperature range 600−680 °C without any experimental evidence of the monoclinic phase in the X-ray diffraction data as shown in Figure 1 (c). This indicates that the substitution of Bi^{3+} and V^{5+} into the A and B site stabilized the tetragonal scheelite phase in KBMV0.82 and KBMV0.85

dx.doi.org/10.1021/ic201862e | Inorg. Chem. 2011, 50, 12733−12738

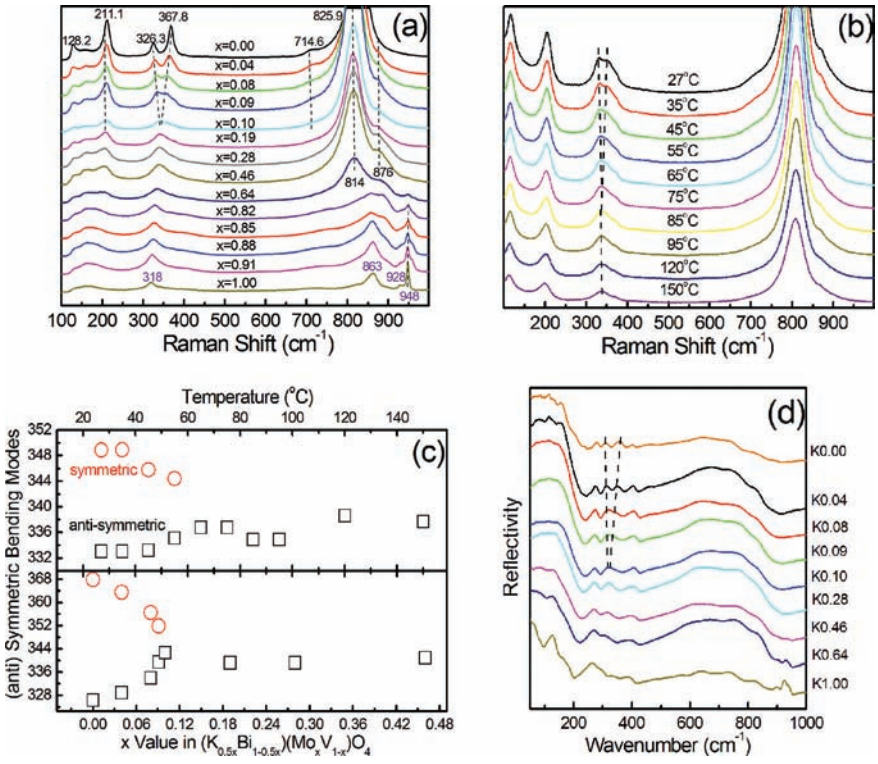

Figure 2. Room temperature Raman spectroscopy of the $(K_{0.5x}Bi_{1-0.5x})(Mo_xV_{1-x})O_4$ ($0.0 \leq x \leq 1.0$) ceramics (a), high temperature Raman spectroscopy for KBMV0.08 (b) and band shift for (anti) symmetric bending mode as a function of temperature (c), and room temperature IR spectra (d).

sample. As shown in Figure 1 (g), the phase diagram of the whole $(K_{0.5x}Bi_{1-0.5x})(Mo_xV_{1-x})O_4$ ($0 \leq x \leq 1.0$) system can be separated into at least six regions in the temperature below the melting points: I, scheelite monoclinic phase ($BiVO_4$ type) region with $0 \leq x < 0.1$; II, scheelite tetragonal phase ($BiVO_4$ type) region with $0.1 \leq x < 0.19$; III, two scheelite tetragonal phases (one is $BiVO_4$ type and the other one is $(KBi)_{1/2}MoO_4$ type) region with $0.1 \leq x < 0.82$; IV, scheelite tetragonal phase solid solution $0.82 \leq x \leq 0.85$ ($(KBi)_{1/2}MoO_4$ type); V, composite phases region with $0.85 < x < 0.88$ ($(KBi)_{1/2}MoO_4$ type tetragonal and monoclinic phases); VI, scheelite monoclinic phase ($(KBi)_{1/2}MoO_4$ type) region with $0.91 \leq x \leq 1.0$.

A series of Raman spectra for the $(K_{0.5x}Bi_{1-0.5x})(Mo_xV_{1-x})O_4$ ($0 \leq x \leq 1.0$) ceramics is shown in Figure 2 (a) over the frequency range 100−1000 cm^{-1}. It is observed that the spectra of pure $BiVO_4$ is dominated by an intense Raman band near 825.9 cm^{-1} assigned to $\nu_s(V-O)$, which is a symmetric V−O stretching mode with A_g symmetry, and with a weak shoulder at about 714.6 cm^{-1} assigned to $\nu_{as}(V-O)$, which is an antisymmetric V−O stretching mode with B_g symmetry. The $\delta_s(VO_4^{3-})$ is the symmetric A_g bending mode of the vanadate anion, and $\delta_{as}(VO_4^{3-})$ is an antisymmetric B_g bending mode associated with the vanadate anion modes and are near 367.8 and 326.3 cm^{-1}, respectively, and external modes (rotation/translation) occur near 211.1 cm^{-1} and 128.2 cm^{-1}, respectively. All results for the Raman peaks are in agreement with the earlier articles.[19−25] It is seen that the most intensive modes $\nu_s(V-O)$ (A_g) gradually shift toward the low wavenumber direction from 825.9 cm^{-1} for $BiVO_4$ to 814 cm^{-1} for NBMV0.64 as the composition varies with the x value increasing from 0.00 to 0.64. Also the average short-range symmetry of the VO_4 tetrahedra becomes more regular,[21−24] as inferred from the full width at half-maximum (fwhm) of the peak increases with composition. As the Mo content increased from $x = 0.00$ to $x = 0.64$, the band around 876 cm^{-1}, which was assigned to $\nu_{as}(MoO_4)$, became stronger and stronger and the mode at 948 cm^{-1} assigned to $\nu_s(MoO_4)$ appeared at $x = 0.64$. For pure monoclinic $(K,Bi)_{1/2}MoO_4$, the strongest band is at 948 cm^{-1} and its shoulder band at 928 cm^{-1} were assigned as a symmetric mode of the terminal bond system ($\nu_s(MoO_4)$). The band at 863 cm^{-1} was assigned to the $\nu_{as}(MoO_4)$ with $\nu(Mo_2O_8)$ bridge vibrations. The band at 320 cm^{-1} originated from symmetric bending vibrations of the MoO_4^{2-} unit and its position is almost exactly the same as for $NaBi(MoO_4)_2$ as analyzed by Hanuza.[26−29] However, the Raman bands are not sensitive to the phase compositions and it is difficult to distinguish among the differing phase regions. It is noticed that with the increase of x value, the symmetric bending modes $\delta_s(VO_4^{3-})$ at 367.8 cm^{-1} red-shifted and the antisymmetric bending modes $\delta_{as}(VO_4^{3-})$ at 326.3 cm^{-1} blueshifted as shown in Figure 2 (a). When x reached 0.10, the symmetric bending modes $\delta_s(VO_4^{3-})$ and the antisymmetric bending modes $\delta_{as}(VO_4^{3-})$ merged into one band, which is in accord to the structural change from monoclinic to tetragonal phase. The in situ Raman spectra of KBMV0.08 sample in the temperature range 27∼150 °C are shown in Figure 2 (b). As the temperature increases, intense of all the Raman bands decreases and the fwhm of the peak increases. The characteristic merging of the symmetric bending modes $\delta_s(VO_4^{3-})$ and the antisymmetric bending modes $\delta_{as}(VO_4^{3-})$ was observed at around 75 °C. The detailed data are shown in Figure 2 (c) and have the similar trend to the situation in composition change. The in situ Raman results also give an evidence for the phase transition in $(K_{0.5x}Bi_{1-0.5x})(Mo_xV_{1-x})O_4$ ($x \leq 0.10$). Figure 2 (d) presents the IR reflectivity spectra of $(K_{0.5x}Bi_{1-0.5x})$-

dx.doi.org/10.1021/ic201862e | Inorg. Chem. 2011, 50, 12733−12738

$(Mo_xV_{1-x})O_4$ ($0.0 \le x \le 1.0$) ceramics. It is seen that the two bands at 309.5 cm^{-1} and 357.2 cm^{-1}, which is assigned to $\delta_{as}(VO_4)$ mode and the $\delta_s(VO_4)$, respectively, moved closer to each other with the increase of x value and finally merged into one band at around x = 0.10. This is similar to the Raman analysis above and also support the compositional phase transition at room temperature.

Figure 3 shows the microwave dielectric permittivity and Qf value of the $(K_{0.5x}Bi_{1-0.5x})(Mo_xV_{1-x})O_4$ ($0 \le x \le 1.0$) ceramics

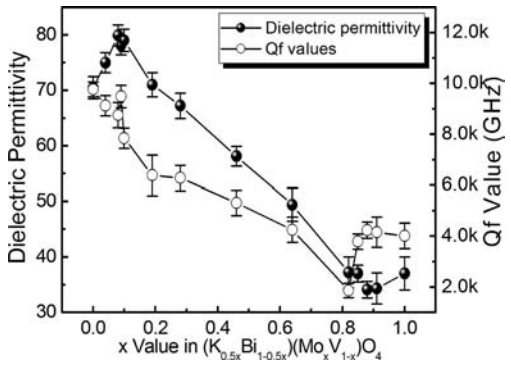

Figure 3. Microwave dielectric permittivity and Qf value of the $(K_{0.5x}Bi_{1-0.5x})(Mo_xV_{1-x})O_4$ ($0 \le x \le 1.0$) ceramics at room temperature as a function of x value (at 3.7−6 GHz).

at room temperature as a function of x value (at 3.7−6 GHz). It is seen that as the x value increases from 0 to around 0.1, the dielectric permittivity increases linearly from 70 to about 80 at the phase boundary of ferroelastic-paraelastic phases, which is similar to the results we found in $(Li_{0.5x}Bi_{1-0.5x})(Mo_xV_{1-x})O_4$ system.[10,11] Then it decreases linearly to a minimum value of 34.2 for KBMV0.88 sample and the end member $(K_{0.5}Bi_{0.5})$-MoO_4 has a relative permittivity about 37. The Qf value almost decreases with x value from about 9700 GHz for pure $BiVO_4$ to a minimum value of 1860 GHz for KBMV0.82, in which a pure secondary tetragonal phase was formed. A slight fluctuation of Qf value was observed at the ferroelastic-paraelastic phase boundary, which may be caused by the phase transition near room temperature.

Due to the ferroelastic-paraelastic phase transition, the temperature coefficient TCF can not be simply characterized by a linear equation. The microwave dielectric permittivity and Qf value of the $(K_{0.5x}Bi_{1-0.5x})(Mo_xV_{1-x})O_4$ ceramics (x = 0.04, 0.08, 0.09, 0.10, 0.19) as a function of temperature in the temperature range 20−150 °C are shown in Figure 4. As predicted by the classical Lyddane-Sach-Teller (LST) relation,[30] any softening of a tranverse optic (TO) mode leads to increase of the relative permittivity, which means there is a maximum value at the phase transition temperature as shown in Figure 4 (a). The phase transition temperatures were plotted as a function of x value in the $(K_{0.5x}Bi_{1-0.5x})(Mo_xV_{1-x})O_4$ ceramics ($x \le 0.10$) and compared with the external pressure induced ones, which are shown in Figure 5. The XRD analysis presented above also provided consistent evidence for the shift of phase transition temperature in the $(K_{0.5x}Bi_{1-0.5x})(Mo_xV_{1-x})$-$O_4$ ceramics.

The phase transition temperature of pure $BiVO_4$ was reported to be about 255 °C. As the x increases to 0.10, the phase transition temperature almost linearly decreases to approximately 42 °C. Earlier, Hazen and Mariathasan[31] showed a linear relationship between transition temperature and

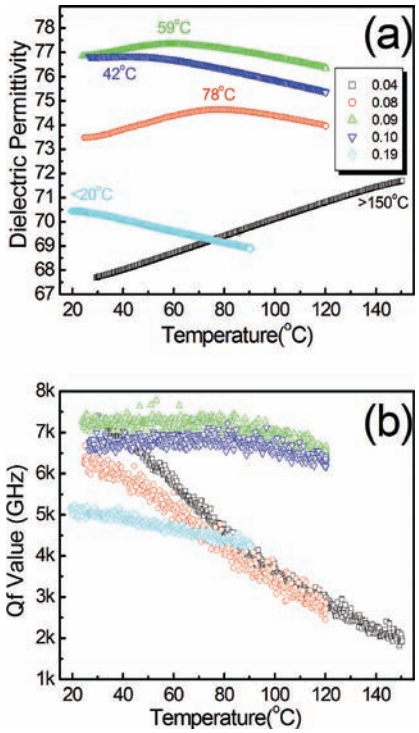

Figure 4. Microwave dielectric permittivity (a) and Qf values (b) of the $(K_{0.5x}Bi_{1-0.5x})(Mo_xV_{1-x})O_4$ (0 = 0.04, 0.08, 0.09, 0.10, and 0.19) ceramics as a function of temperature (in range 20−150 °C).

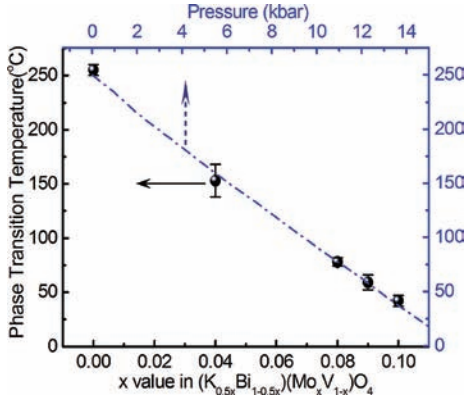

Figure 5. Ferroelastic phase transition (monoclinic to tetragonal structure) temperature of the $(K_{0.5x}Bi_{1-0.5x})(Mo_xV_{1-x})O_4$ ($0 \le x \le 0.10$) ceramics as a function of x value and pressure (data from ref 31.).

pressure as follows:

$$T(K) = 250(\pm 3) - 15.0(\pm 3)P(kbar) \quad (2)$$

A linear relationship between transition temperature and x value can also be obtained as follows in the range of $x \le 0.10$:

$$T(K) = 252(\pm 4) - 2140(\pm 30)x \quad (3)$$

These two relationships give the phase stability of the $BiVO_4$, as related to the monoclinic phase under different variables, namely pressure and composition. These two relationships also help to understand the phase transition. In $(K_{0.5x}Bi_{1-0.5x})$-$(Mo_xV_{1-x})O_4$, on the A-site, 8-coordinated Bi^{3+} and K^+ atoms have a radius of 1.17 Å and 1.51 Å, respectively. On the B-site, 4-coordinated V^{5+} and Mo^{6+} cations have a radius of 0.355 Å

dx.doi.org/10.1021/ic201862e | Inorg. Chem. 2011, 50, 12733−12738

and 0.41 Å, respectively, according to Shannon's data.[32] As x value increases, the substitution of K^+ on the A site for Bi^{3+} and Mo^{6+} on the B site for V^{5+} significantly increased the space occupancy and gave much internal pressure to lead the crystal structure transition from monoclinic to tetragonal structure, which has the similar influence of external pressure. Hence, it is understandable that the composition and the external pressure variety on the $(K_{0.5x}Bi_{1-0.5x})(Mo_xV_{1-x})O_4$ system result are consisten with displacive phase transition.

CONCLUSIONS

The phase diagram of the whole $(K_{0.5x}Bi_{1-0.5x})(Mo_xV_{1-x})O_4$ ($0 \leq x \leq 1.0$) system can be separated into at least six regions in the temperature below the melting points: I, scheelite monoclinic phase ($BiVO_4$ type) region with $0 \leq x < 0.1$; II, scheelite tetragonal phase ($BiVO_4$ type) region with $0.1 \leq x < 0.19$; III, two scheelite tetragonal phases (one is $BiVO_4$ type and the other one is $(KBi)_{1/2}MoO_4$ type) region with $0.1 \leq x < 0.82$; IV, scheelite tetragonal phase solid solution $0.82 \leq x \leq 0.85$ ($(KBi)_{1/2}MoO_4$ type); V, composite phases region with $0.85 < x < 0.88$ ($(KBi)_{1/2}MoO_4$ type tetragonal and monoclinic phases); VI, scheelite monoclinic phase ($(KBi)_{1/2}MoO_4$ type) region with $0.91 \leq x \leq 1.0$. From the high temperature XRD analysis, the ferroelastic-paraelastic phase transition in the $(K_{0.5x}Bi_{1-0.5x})(Mo_xV_{1-x})O_4$ ($0 \leq x \leq 1.0$) system can shifted from 255 °C for pure $BiVO_4$ to about 42 °C for KBMV0.10 sample with compositional variation. A peak value of dielectric permittivity was observed at the phase transition temperature for $(K_{0.5x}Bi_{1-0.5x})(Mo_xV_{1-x})O_4$ ($0 < x \leq 0.10$) samples, consistent with a soft mode softening. High dielectric permittivity above 78 and Qf value above 7800 GHz were obtained in $(K_{0.5x}Bi_{1-0.5x})(Mo_xV_{1-x})O_4$ ($0.8 \leq x \leq 0.10$) samples at room temperature.

AUTHOR INFORMATION

Corresponding Author

*Phone: +86-29-82668679. Fax: +86-29-82668794. E-mail: zhoudi1220@gmail.com.

ACKNOWLEDGMENTS

This work was supported by the National 973-project of China (2009CB623302), headmaster foundation of Xi'an Technological University (XAGDXJJ1001), NSFC projects of China (60871044, 50835007), the National Science Foundation I/UCRC program and the Fundamental Research Funds for the Central University. We thank Qiu-Ping Wang, Han-Chen Liu, Chao Zhou, Xiao-Hui Song, Yu-Yin Wang, Tao Shao, and Ze-Ming Qi for their help in Raman, UV and IR experimental. We also thank the administrators in IR beamline workstation of National Synchrotron Radiation Laboratory (NSRL) for their help in the IR measurement.

REFERENCES

(1) Cava, R. J. *J. Mater. Chem.* **2001**, *11*, 54.
(2) Feteira, A.; Sinclair, D. C. *J. Mater. Chem.* **2009**, *19*, 356.
(3) Sebastian, M. T.; Jantunen, H. *Int. Mater. Rev.* **2008**, *53*, 57.
(4) Blin, J. L.; LorriauxRubbens, A.; Wallart, F.; Wignacourt, J. P. *J. Mater. Chem.* **1996**, *6*, 385.
(5) Valant, M.; Suvorov, D. *J. Am. Ceram. Soc.* **2000**, *83*, 2721.
(6) Wee, S. H.; Kim, D. W.; Yoo, S. I. *J. Am. Ceram. Soc.* **2004**, *87*, 871.
(7) Zhou, D; Randall, C. A.; Wang, H.; Pang, L. X.; Yao, X. *J. Am. Ceram. Soc.* **2010**, *93*, 2147.
(8) Klevtsov, P. V.; Vinokurov, V. A.; Klevtsova, R. F. *Sov. Phys. Crystallogr.* **1974**, *18*, 749.
(9) Zhou, D.; Randall, C. A.; Pang, L. X.; Wang, H.; Guo, J.; Zhang, G. Q.; Wu, Y.; Shui, L.; Yao, X. *Mater. Chem. Phys.* **2011**, *129*, 688.
(10) Zhou, D.; Qu, W. G.; Randall, C. A.; Pang, L. X.; Wang, H.; Wu, X. G.; Guo, J.; Zhang, G. Q.; Shui, L.; Wang, Q. P.; Liu, H. C.; Yao, X. *Acta Mater.* **2011**, *59*, 1502.
(11) Zhou, D.; Randall, C. A.; Wang, H.; Pang, L. X.; Yao, X. *J. Am. Ceram. Soc.* **2010**, *93*, 2147.
(12) Bierlein, J. D.; Sleight, A. W. *Solid State Commun.* **1975**, *16*, 69.
(13) David, W. I. F.; Glazer, A. M.; Hewat, A. W. *Phase Transitions* **1979**, *1*, 155.
(14) Sleight, A. W.; Chen, H. Y.; Ferretti, A.; Cox, D. E. *Mater. Res. Bull.* **1979**, *14*, 1571.
(15) Kisel, N. G.; Mokhosoev, M. V. *Ukr. Khim. Zh.* **1972**, *38*, 743.
(16) Klevtsov, P. V.; Vinokurov, V. A.; Klevtsova, R. F. *Kristallografiya* **1973**, *18*, 1192.
(17) Klevtsov, P. V.; Vinokurov, V. A. *Kristallografiya* **1974**, *19*, 763.
(18) Klevtsov, P. V.; Vinokurov, V. A. *Sov. Phys. Crystallogr.* **1975**, *19*, 474.
(19) Frost, R. L.; Henry, D. A.; Weier, M. L.; Martens, W. J. *Raman Spectrosc.* **2006**, *37*, 722.
(20) Jang, M. S.; Park, H. L.; Kim, J. N.; Ro, J. H.; Park, Y. H. *Jpn. J. Appl. Phys.* **1985**, *24*, 506.
(21) Hardcastle, F. D.; Wachs, I. E.; Eckert, H.; Jefferson, D. A. *J. Solid State Chem.* **1991**, *90*, 194.
(22) Zhang, A.; Zhang, J.; Cui, N.; Tie, X.; An, Y.; Li, L. *J. Mol. Catal. A: Chem.* **2009**, *304*, 28.
(23) Yu, J.; Kudo, A. *Adv. Funct. Mater.* **2006**, *16*, 2163.
(24) Hardcastle, F. D.; Wachs, I. E. *J. Phys. Chem.* **1991**, *95*, 503.
(25) Zhang, H. M.; Liu, J. B.; Wang, H.; Zhang, W. X.; Yan, H. *J. Nanopart. Res.* **2008**, *10*, 767.
(26) Weinstock, N.; Schulze, H.; Muller, A. *J. Chem. Phys.* **1973**, *59*, 5063.
(27) Hanuza, J.; Mqczka, M.; Macalik, L.; Maas, J. *J. Mol. Struct.* **1994**, *325*, 119.
(28) Hanuza, J.; Maczka, M.; Vandermaas, J. H. *Vib. Spectrosc.* **1995**, *8*, 417.
(29) Hanuza, J.; Maczka, M.; Macalik, L.; Vandermaas, J. H. J. *Mol. Struct.* **1994**, *325*, 119.
(30) Lyddane, R. H.; Sachs, H.; Tellar, E. *Phys. Rev.* **1941**, *59*, 673.
(31) Hazen, R. M.; Mariathasan, J. W. E. *Science* **1982**, *216*, 991.
(32) Shannon, R. D. *Acta Crystallogr.* **1976**, *A32*, 751.